Terahertz wavefront measurement with a Hartmann sensor

H. Richter, M. Greiner-Bär, N. Deßmann, J. Pfund, M. Wienold et al.

Citation: Appl. Phys. Lett. **101**, 031103 (2012); doi: 10.1063/1.4737164
View online: http://dx.doi.org/10.1063/1.4737164
View Table of Contents: http://apl.aip.org/resource/1/APPLAB/v101/i3
Published by the American Institute of Physics.

Terahertz wavefront measurement with a Hartmann sensor

H. Richter,[1,a)] M. Greiner-Bär,[1] N. Deßmann,[1] J. Pfund,[2] M. Wienold,[3] L. Schrottke,[3] R. Hey,[3] H. T. Grahn,[3] and H.-W. Hübers[1,4]
[1]*German Aerospace Center (DLR), Institute of Planetary Research, Rutherfordstr. 2, 12489 Berlin, Germany*
[2]*Optocraft GmbH, Am Weichselgarten 7, 91058 Erlangen, Germany*
[3]*Paul-Drude-Institut für Festkörperelektronik, Hausvogteiplatz 5-7, 10117 Berlin, Germany*
[4]*Institut für Optik und Atomare Physik, Technische Universität Berlin, Hardenbergstraße 36, 10623 Berlin, Germany*

(Received 30 May 2012; accepted 28 June 2012; published online 17 July 2012)

The measurement of the wavefront of a terahertz (THz) beam is essential for the development of any optical instrument operating at THz frequencies. We have realized a Hartmann wavefront sensor for the THz frequency range. The sensor is based on an aperture plate consisting of a regular square pattern of holes and a microbolometer camera. The performance of the sensor is demonstrated by characterizing the wavefront of a THz beam emitted by a quantum-cascade laser. The wavefront determined by the sensor agrees well with that expected from a Gaussian-shaped beam. The spatial resolution is 1 mm, and a single-wavefront measurement takes less than 1 s.
 [http://dx.doi.org/10.1063/1.4737164]

Ongoing progress in the development of terahertz (THz) systems has enabled a wide variety of research applications as well as commercial applications. Independent of the application of a THz system (either for imaging or for spectroscopy), its performance depends to a large extent on the quality of the optical layout. For the design of any optical system, the knowledge of the intensity and phase distribution of the beam at any location in the system is essential. Usually, a THz optical system is designed for the fundamental Gaussian beam. The measurement of the intensity and phase of this beam at one location in the system allows for the calculation of both at any other location with high precision. Usually, the intensity distribution within a THz beam is measured by either scanning a single pixel detector such as a Golay cell or a pyroelectric detector across the beam.[1] Alternatively, an array detector such as a pyroelectric camera or a microbolometer array can be used, and time-consuming scanning is not required anymore.[2] In this way, the intensity distribution is measured with a high accuracy and spatial resolution. While this measurement already provides important information, the fact that the phase distribution is missing limits the determination of the beams geometric parameters and its propagation properties.

The Hartmann plate is a simple and elegant means for measuring the shape of a wavefront. It was proposed by Hartmann (cf., Ref. 3). The concept of this sensor is based on measuring the aberrations of a wavefront that passes through a screen of small apertures. The resulting image is a spatial decomposition of the incoming wavefront into a number of points, which is equal to the number of apertures in the screen. Each point is the diffracted image of a specific zone of the incoming wavefront. If a perfect plane wave is diffracted by the Hartmann plate, the resulting image is composed of an array of points, which has the same spacing as the array of apertures on the plate. A non-planar wavefront will result in a distorted image. The measurement of the differences between the spot positions originating from a perfect plane wave and those from the unknown wavefront allows for the calculation of the local slope, at which the wavefront intersects each aperture of the Hartmann plate. Thus, the phase information is translated into an intensity measurement, from which the wavefront can be calculated.

To overcome the limitations of present beam measurement techniques at THz frequencies, namely the lack of phase information, we combine a Hartmann plate with a microbolometer camera. This allows for the determination of the phase and intensity distribution of a THz beam. As a first demonstration of its performance, the Hartmann sensor is applied to characterize a beam emitted by a THz quantum-cascade laser (QCL).

The configuration of the measurement setup is illustrated in Fig. 1. The main items of the wavefront sensor are a metal plate with an array of holes, which acts as the Hartmann plate, and an uncooled infrared camera (InfraTec

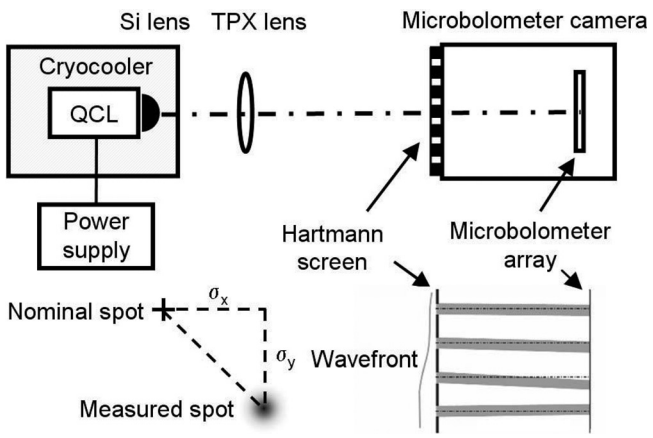

FIG. 1. Top: in the measurement setup, the QCL beam is focused with a combination of a Si lens (inside the cryocooler) and a TPX lens. After passing through a Hartmann plate, it is detected with a microbolometer camera. Bottom right: expanded view of the wavefront impinging onto the Hartmann plate. Bottom left: illustration of the geometry used for the data analysis.

[a)]Electronic mail: Heiko.Richter@dlr.de.

GmbH, VarioCAM),[4] which images the diffraction pattern behind the plate. The Hartmann plate consists of a regular square pattern of holes with a diameter $d = 0.5$ mm and a spacing $g = 1$ mm. The hole pattern is drilled into an aluminium plate with a thickness $t = 1$ mm. Such a plate acts as a high-pass filter with a cut-off frequency $\nu_{co} = 0.586\ c/d = 0.18$ THz (c refers to the speed of light),[5] which is well below the THz frequencies of interest. The transmittance of the plate shown in Fig. 2 was measured with a Fourier transform spectrometer. The low-frequency cut-off occurs at approximately 0.25 THz, while the maximum transmittance is observed at 0.33 THz. Toward higher frequencies, the transmission decreases and reaches a minimum at approximately 1.4 THz. This corresponds to the frequency where the zeroth-order transmitted beam of one hole interferes destructively with the first-order diffracted beam from the neighboring holes. With a further increase of the frequency, i.e., when the wavelength of the incident wave becomes smaller than the hole diameter, diffraction becomes less important, and the transmittance T approaches the geometrical limit determined by the relative area occupied by the holes, which is $T = \pi d^2/(4g^2) = 0.2$. Similar plates with $d = 1$ mm and $g = 2$ mm as well as $d = 2$ mm and $g = 4$ mm were also investigated. At 3.1 THz, the frequency of the QCL which is analyzed, the plate shown in the inset of Fig. 2 yields the best results, because its transmission is high and diffraction is still significant.

The camera used for the Hartmann sensor is equipped with a microbolometer array made from amorphous silicon. The array is a matrix of 640×480 pixels with a pixel pitch of 25 μm. The camera is optimized for wavelengths of 8 to 14 μm. In order to improve its sensitivity at THz frequencies, the germanium objective lens in front of the camera is removed. The wavefront plate is mounted directly onto the camera approximately at the position of the objective lens. The distance between the plate and the microbolometer array amounts to 24 mm. The images were recorded with the 50 Hz frame rate of the camera. For improving the signal-to-noise ratio (SNR), 50 images were averaged.

For a demonstration of the performance of the Hartmann sensor, the beam of a THz QCL was investigated. THz QCLs are radiation sources with a large potential for research applications as well as for commercial applications, because they exhibit excellent radiation properties and they are compact and easy to use. The laser employed in this experiment operates at 3.1 THz in continuous-wave mode.[6] It consists of a 1.16-mm long Fabry-Pérot cavity and a single plasmon (SP) waveguide. Further details of the performance of the QCL can be found in Ref. 7. The QCL is mounted onto the cold finger of a mechanical cryocooler, which has a heat extraction of 1 W at 4 K. Since the input power of the laser amounts to 4.4 W, the smallest achievable temperature during laser operation is 20 K. The driving current for the QCL is supplied by a battery-driven current source. The maximum output power is approximately 2 mW. The beam from the QCL is focused with a 6-mm diameter hemispherical silicon lens inside the cryocooler right after the output facet of the QCL and another lens (focal length 65 mm) made from polymethylpentene (PMP, trade mark TPX) on the outside. This lens combination forms an almost Gaussian-shaped beam waist at a distance of 120 mm from the TPX lens.

The beam profile and the diffraction pattern generated by the Hartman plate were measured with the microbolometer camera at a distance of 180 mm from the TPX lens and are shown in Figs. 3(a) and 3(b), respectively. At this distance, the beam is slightly divergent. The beam profile deviates somewhat from a Gaussian shape because the QCL itself emits an asymmetric beam profile and the Si lens does not correct this completely.[8] The area of the Hartmann plate which is illuminated by the THz beam corresponds to approximately 130 holes. Because there are no focusing elements between the Hartmann plate and the microbolometer

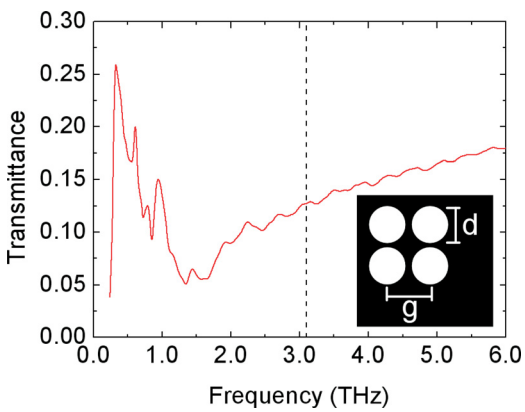

FIG. 2. Transmittance vs. frequency of the aperture screen with $d = 0.5$ mm and $g = 1$ mm used for the Hartmann sensor. The inset shows the geometry of the Hartmann plate. The dashed line indicates the frequency of the investigated QCL.

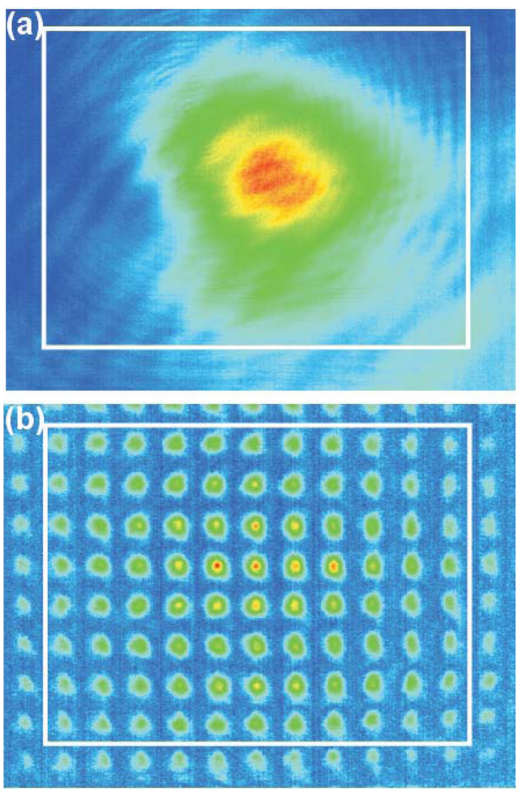

FIG. 3. (a) Beam profile (640×480 pixels) and (b) spot pattern generated by the Hartman plate, both measured with a microbolometer camera. The white frames indicate the area which was used for the reconstruction of the wavefront.

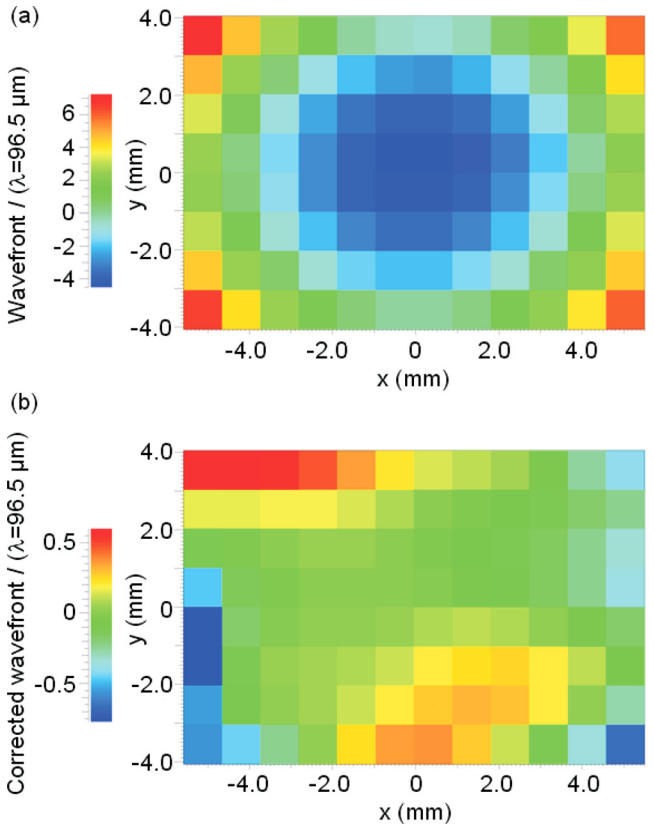

FIG. 4. (a) Calculated wavefront and (b) and corrected wavefront. The small, asymmetric aberrations indicate systematic alignment errors between the laser beam and the Hartmann sensor.

array, the spots on the array are somewhat blurry. Nevertheless, the image quality is sufficient for determining their spatial centroids. In total, 130 spots are detected by the camera. Out of these, 96 were used for the analysis of the wavefront. The area which is analyzed is indicated by the white frames in Figs. 3(a) and 3(b). The outer spots are either incomplete or too much out of focus for any further analysis. The analysis and the calculation of the wavefront were performed using the commercial software SHSWorks Basic from Optocraft.[9] This software determines the geometrical position of each spot in the plane of the microbolometer array from a calculation of its centroid taking into account the intensity of each pixel in the spot. In this way, we determine the displacement relative to the nominal spot position, i.e., the position of the spot for a plane wave, as indicated by σ_x and σ_y in the lower left part of Fig. 1. From this displacement, we calculate the slopes, which in turn allows for the reconstruction of the wavefront using an iterative reconstruction algorithm.[10,11] The wavefront can be represented by a linear combination of Zernike polynomials.[12] The calculated wavefront is shown in Fig. 4(a). Subtraction of the second order alignment terms of the Zernike polynomials (i.e., tilt and defocus) from the wavefront yields the so called corrected wavefront (Fig. 4(b)). The wavefront in Fig. 4(a) is symmetric in both directions, but elongated by about a factor of 1.2 in the x direction compared to the y direction. At the positions $x = 0$ mm and $y = \pm 4$ mm as well as $x = \pm 4$ mm and $y = 0$ mm, the wavefront deviates by approximately five wavelengths from the wavelength at the central point. This deviation increases to about ten wavelengths in the corners ($x = \pm 4$ mm and $y = \pm 4$ mm). The small, asymmetric aberrations of ± 0.6 wavelengths for the corrected wavefront indicate systematic alignment errors between the laser beam and the Hartmann sensor.

In summary, a Hartmann sensor consisting of an aperture plate and a microbolometer camera has been realized. The measurement of a beam from a THz QCL demonstrates that the reconstruction of a wavefront is readily possible. The wavefront determined by this method agrees well with the expectation of an almost Gaussian-shaped wavefront. Several improvements can be envisaged. First of all, the Hartmann plate might be replaced by a microlens array, which transforms it into a Shack-Hartmann sensor.[13] This will improve the SNR for each spot as well as the determination of the spot position. Second, the SNR might also be improved by using a dedicated THz microbolometer camera, which have been recently become available.[14] Third, the spatial resolution can be improved by increasing the density of the apertures or microlenses. With these improvements, an easy-to-handle THz wavefront sensor with video-rate capability becomes feasible.

This work was supported in part by the European Commission through the ProFIT program of the Investitionsbank Berlin.

[1]H. Richter, A. D. Semenov, S. G. Pavlov, L. Mahler, A. Tredicucci, H. E. Beere, D. A. Ritchie, K. Il'in, M. Siegel, and H.-W. Hübers, Appl. Phys. Lett. **93**, 141108 (2008).
[2]A. W. M. Lee, Q. Qin, S. Kumar, B. S. Williams, Q. Hu, and J. L. Reno, Appl. Phys. Lett. **89**, 141125 (2006).
[3]J. Hartmann, Z. Instrumentenk. **20**, 47 (1900).
[4]E. Bründermann, J. Ränsch, M. Krauß, and J. Kunsch, Photonik **38**(6), 60 (2006).
[5]F. Keilmann, Int. J. Infrared Millim Waves **2**, 259 (1981).
[6]M. Wienold, L. Schrottke, M. Giehler, R. Hey, W. Anders, and H. T. Grahn, Electron. Lett. **45**, 1030 (2009).
[7]H. Richter, M. Greiner-Bär, S. G. Pavlov, A. D. Semenov, M. Wienold, L. Schrottke, M. Giehler, R. Hey, H. T. Grahn, and H.-W. Hübers, Opt. Express **18**, 10177 (2010).
[8]H.-W. Hübers, S. G. Pavlov, A. D. Semenov, R. Köhler, L. Mahler, A. Tredicucci, H. E. Beere, D. A. Ritchie, and E. H. Linfield, Opt. Express **13**, 5890 (2005).
[9]Supplemental material to "SHSLab – High performance wavefront sensor system", Optocraft GmbH (2011).
[10]W. H. Southwell, J. Opt. Soc. Am. **70**, 998 (1980).
[11]H. Sickinger, O. Falkenstörfer, N. Lindlein, and J. Schwider, Opt. Eng. **33**, 2680 (1994).
[12]M. Born and E. Wolf, *Principles of Optics*, 7th ed. (Cambridge University Press, 1999).
[13]R. V. Shack and B. C. Platt, J. Opt. Soc. Am. **61**, 656 (1971).
[14]N. Oda, M. Sano, K. Sonoda, H. Yoneyama, S. Kurashina, M. Miyoshi, T. Sasaki, I. Hosako, N. Sekine, T. Sudou, and S. Ohkubo, Proc. SPIE **8012**, 80121B (2011).